



# The use of novel biodegradable, optically active and nanostructured poly(amide-ester-imide) as a polymer matrix for preparation of modified ZnO based bionanocomposites

Amir Abdolmaleki<sup>a,c,\*</sup>, Shadpour Mallakpour<sup>b,c,\*\*</sup>, Sedigheh Borandeh<sup>a</sup>

<sup>a</sup> Department of Chemistry, Isfahan University of Technology, Isfahan 84156-83111, Islamic Republic of Iran

<sup>b</sup> Organic Polymer Chemistry Research Laboratory, Department of Chemistry, Isfahan University of Technology, Isfahan 84156-83111, Islamic Republic of Iran

<sup>c</sup> Nanotechnology and Advanced Materials Institute, Isfahan University of Technology, Isfahan 84156-83111, Islamic Republic of Iran

## ARTICLE INFO

### Article history:

Received 20 November 2011

Received in revised form 12 January 2012

Accepted 14 February 2012

Available online 22 February 2012

### Keywords:

A. Nanostructures

A. Composites

C. Electron microscopy

C. Differential scanning calorimetry (DSC)

C. Thermogravimetric analysis (TGA)

## ABSTRACT

A novel biodegradable and nanostructured poly(amide-ester-imide) (PAEI) based on two different amino acids, was synthesized via direct polycondensation of biodegradable *N,N'*-bis[2-(methyl-3-(4-hydroxyphenyl)propanoate)]isophthaldiamide and *N,N'*-(pyromellitoyl)-bis-*L*-phenylalanine diacid. The resulting polymer was characterized by FT-IR, <sup>1</sup>H NMR, specific rotation, elemental analysis, thermogravimetric analysis (TGA), differential scanning calorimetry (DSC), X-ray diffraction (XRD) and field emission scanning electron microscopy (FE-SEM) analysis. The synthesized polymer showed good thermal stability with nano and sphere structure. Then PAEI/ZnO bionanocomposites (BNCs) were fabricated via interaction of pure PAEI and ZnO nanoparticles. The surface of ZnO was modified with two different silane coupling agents. PAEI/ZnO BNCs were studied and characterized by FT-IR, XRD, UV/vis, FE-SEM and TEM. The TEM and FE-SEM results indicated that the nanoparticles were dispersed homogeneously in PAEI matrix on nanoscale. Furthermore the effect of ZnO nanoparticle on the thermal stability of the polymer was investigated with TGA and DSC technique.

© 2012 Elsevier Ltd. All rights reserved.

## 1. Introduction

Controlled patterning of materials at the nanoscale is the bases for nanotechnological manufacturing. Recently, several nanostructured polymers have been fabricated for an extensive range of potential applications [1,2]. The development of nanostructured polymers has made widely essential and practical frontiers, which has attracted excellent attention in the last decades [3]. Furthermore, with the expansion of nanotechnology, nanoparticles have been increasingly applied to organic polymers. These polymeric nanocomposites, in which polymers provide as hosts for inorganic nanoparticles, have attracted scientific and technological interest due to their relatively remarkable various properties including mechanical properties, such as scratching and abrasion resistance, optical properties, and wide-spread potential applications [4–10].

Nanoparticles can be directly added into organic polymers; however, their advantages have been limited due to their aggregation and incompatibility with organic polymers. Consequently, nanoparticles require some modification to turn their surface from hydrophilic to organophilic [11,12]. Nanoparticle modifications have done with different compounds like, surface-active agent, coupling agent, fatty acid and alcohol [13–16].

Nowadays, great interest attracted to nanocomposite based on biopolymers due to their similarity to natural materials [17,18]. Polymers containing amino acids are great candidate for preparing of nanocomposites, because they are biodegradable and biocompatible in the biological environment [19–22] and also can chemically bind with inorganic components of composite materials and consequently stabilize the dispersed additives at a nanoscale level [23,24]. In addition, some of the nanoparticles like ZnO, due to their biological properties like antimicrobial activities, causing biomedical applications for nanocomposites based on them [25,26].

In this investigation, a novel optically active, biodegradable and nanostructured poly(amide-ester-imide) (PAEI) with good thermal stability, was prepared, via direct polycondensation of optically active *L*-phenyl aniline based diacid and an optically active *S*-tyrosine based diol using TsCl/DMF/Py as a condensing agent. Then, poly(amide-ester-imide)/zinc oxide (PAEI/ZnO) bionanocomposites (BNCs) were synthesized under ultrasonic irradiation. The ZnO nanoparticles were functionalized with two different

\* Corresponding author at: Department of Chemistry, Isfahan University of Technology, Isfahan 84156-83111, Islamic Republic of Iran. Tel.: +98 3113912351; fax: +98 3113912350.

\*\* Corresponding author at: Organic Polymer Chemistry Research Laboratory, Department of Chemistry, Isfahan University of Technology, Isfahan 84156-83111, Islamic Republic of Iran. Tel.: +98 3113913267; fax: +98 3113912350.

E-mail addresses: [abdolmaleki@cc.iut.ac.ir](mailto:abdolmaleki@cc.iut.ac.ir), [amirabdolmaleki@yahoo.com](mailto:amirabdolmaleki@yahoo.com) (A. Abdolmaleki), [mallak@cc.iut.ac.ir](mailto:mallak@cc.iut.ac.ir), [mallak777@yahoo.com](mailto:mallak777@yahoo.com), [mallakpour84@alumni.ufl.edu](mailto:mallakpour84@alumni.ufl.edu) (S. Mallakpour).

silane coupling agents for homogeneous dispersing in polymer matrix. The resulting BNCs were characterized by a variety of techniques including FT-IR, XRD, TGA, DSC, UV/vis and their morphology were investigated by FE-SEM and TEM analyses.

## 2. Experimental

### 2.1. Materials

S-Tyrosine, *l*-phenyl aniline, isophthaloyl dichloride,  $\gamma$ -methacryloxypropyltrimethoxy silane, KH570 and  $\gamma$ -aminopropyltriethoxy silane, KH550 were purchased from Merck Chemical Co. *N*-Methyl-2-pyrrolidinon (NMP, Merck Chemical Co.), *N,N*-dimethyl formamide (DMF, Merck Chemical Co.) and triethylamine (TEA, Merck Chemical Co.) were dried over BaO and then were distilled under reduced pressure and stored over 4 Å molecular sieves. ZnO nanoparticle with an average particle size of about 25–30 nm was purchased from Neutrino Co. Other reagents and solvents were obtained commercially and used as received.

### 2.2. Apparatus

A horn probe MISONIX ultrasonic liquid processor, XL-2000 SERIES with frequency  $2.25 \times 10^4$  Hz and power 100 W was used in solution mixture.

### 2.3. Characterization methods

The chemical composition of the intermediates and obtained particles was studied by FT-IR spectroscopy using a Jasco-680 FT-IR spectrophotometer in the spectral range between 4000 and  $400 \text{ cm}^{-1}$  with KBr pellet. Vibration bands were reported as wave number ( $\text{cm}^{-1}$ ). The band intensities are assigned as weak (w), medium (m), shoulder (sh), strong (s), and broad (br). The  $^1\text{H}$  NMR spectrum was recorded on Bruker Advance 500 MHz spectrometer operating on monomers and polymer solution in  $\text{DMSO-}d_6$ . Chemical shifts are given in the  $\delta$  scale in parts per million (ppm). Proton resonances are designated as singlet (s), broad doublet (bd), broad triplet (bt) and multiplet (m). Elemental analyses were performed with a CHNS-932, Leco. Inherent viscosities of polymer solution (0.5%, w/v) in NMP were determined at 25 °C by a standard procedure using a Cannon-Fenske routine viscometer. The specific rotations were measured by a Jasco polarimeter. X-ray diffraction studies of the samples were carried out by Bruker, D8ADVANCE with a scanning rate of  $0.02^\circ/\text{min}$  with  $\text{Cu K}\alpha$  radiation operating at 45 kV and 100 mA within a scan range of  $2\theta = 10\text{--}80^\circ$ . UV/vis spectra of the polymer and PAEI/ZnO BNCs were measured on UV/Vis/NIR spectrophotometer, JASCO, V-570 with solid pellets sample of polymer and BNCs in the spectral range between 200 and 800 nm.

Thermal properties of the polymer and PAEI/ZnO BNCs were studied on STA503 win TA instrument in nitrogen atmosphere at a heating rate of  $10^\circ\text{C}/\text{min}$ . Differential scanning calorimetry (DSC) analysis was taken by Perkin-Elmer DSC-7 in nitrogen atmosphere at a heating rate of  $10^\circ\text{C}/\text{min}$ . The morphology of the synthesized polymer and BNCs was observed using field emission scanning electron microscopy (FE-SEM). FE-SEM micrographs of samples were taken on a Hitachi (S-4160). The morphology and dispersity analysis was performed on transmission electron micrograph (TEM) analyzer on Philips CM 120 operating at 100 kV.

### 2.4. Diol synthesis

*N,N'*-Bis[2-(methyl-3-(4-hydroxyphenyl)propanoate)]i-sophthaldiamide (**5**) was synthesized via the reaction of *S*-tyrosine methyl ester (**3**) [27] (1.07 g, 5.5 mmol) and isophthaloyl dichloride (**4**) (0.5 g, 2.5 mmol) in 6 mL of NMP as a solvent at  $-20^\circ\text{C}$  (Scheme 1) [21].

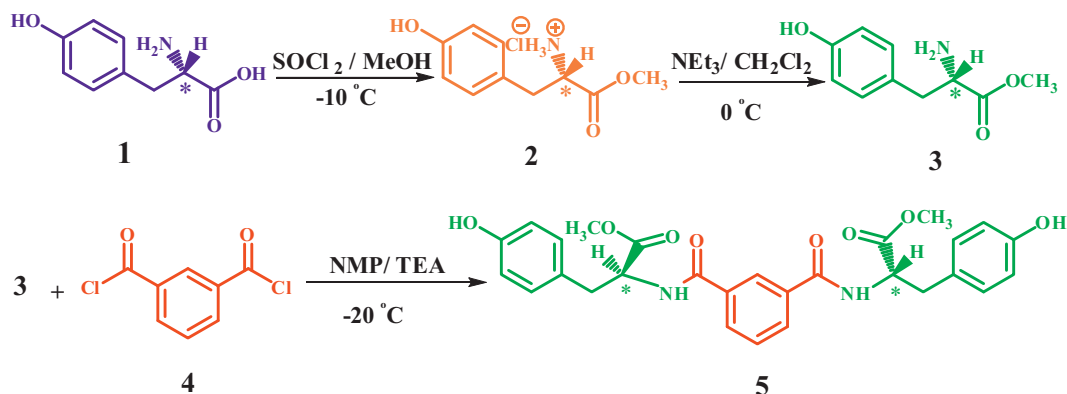
### 2.5. Diacid synthesis

*N,N'*-(Pyromellitoyl)-bis-*l*-phenylalanine diacid (**9**) was prepared according to our previous works [28] and is shown in Scheme 2.

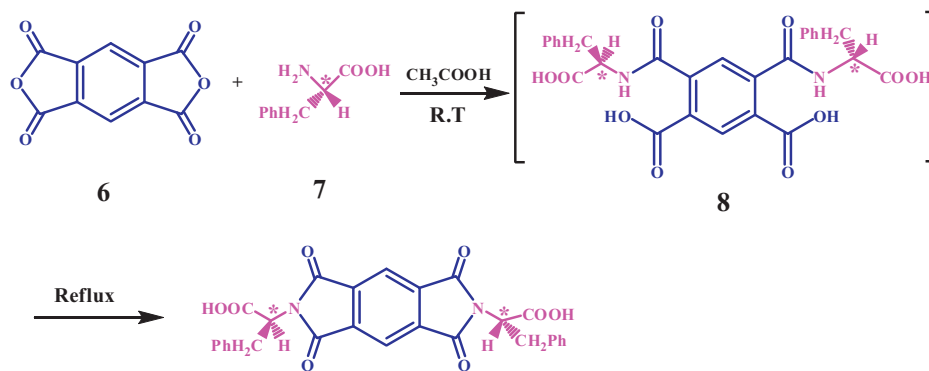
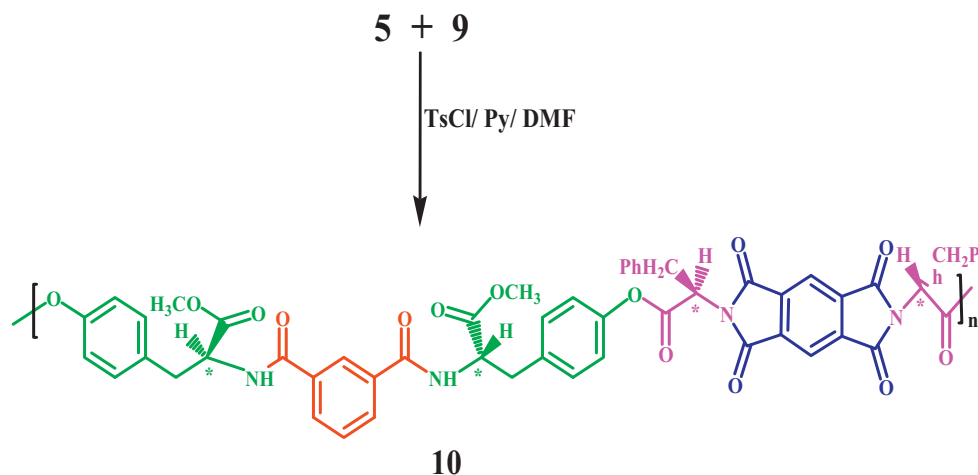
### 2.6. Polymer synthesis

The PAEI was prepared by the following procedure (Scheme 3): a solution of pyridine (Py) (0.4 mL; 5 mmol) with *p*-toluenesulfonyl chloride (TsCl) (0.372 g; 1.95 mmol) after 30 min stirring at room temperature, was treated with DMF (0.18 mL; 2.44 mmol) for 30 min and the mixture was added dropwise to a solution of diacid (**9**) (0.20 g; 0.39 mmol) in Py (0.4 mL). The mixture was maintained at room temperature for 30 min and then diol (**5**) (0.20 g; 0.39 mmol) was added and the whole solution was stirred at room temperature for 30 min and then at  $120^\circ\text{C}$  for 6 h. The viscous liquid was precipitated in 50 mL of methanol/water mixture, filtered off, and washed with methanol/water solution mixture. Powdered polymer was dried at  $80^\circ\text{C}$  for 12 h under vacuum to leave 0.264 g (68%) of cream PAEI.

$[\alpha]_D^{25} = -8.76^\circ$  ( $c = 0.5 \text{ g/dL}$ , NMP); FT-IR (KBr,  $\text{cm}^{-1}$ ):  $\nu = 3374$  (m, br), 1771 (w), 1721 (s), 1649 (m), 1515 (m, sh), 1444 (w), 1385 (m), 1362 (m), 1221 (m), 1106 (m), 828 (w), 727 (m), 700 (m), 491 (w);  $^1\text{H}$  NMR (500 MHz,  $\text{DMSO-}d_6$ , ppm):  $\delta = 2.95$  (m, 4H), 3.28 (m, 4H), 3.57 (s, 6H), 4.62 (m, 2H, chiral center), 4.53 (m, 2H, chiral center), 6.59 (bt, 2H), 6.96 (bd, 4H), 7.02–7.08 (bt, 4H), 7.12 (bd, 4H), 7.29 (bd, 4H), 7.49–7.50 (bt, 1H), 7.87 (bd, 2H), 8.11 (s, 1H), 8.18 (s, 2H) and 8.97 (NH, s, 2H). Elemental analysis for



Scheme 1. Synthesis of diol 5.

Scheme 2. Synthesis of diacid **9**.Scheme 3. Direct polycondensation of diol **5** with diacid **9**.

(C<sub>56</sub>H<sub>44</sub>N<sub>4</sub>O<sub>14</sub>): Calcd: C, 67.46%; H, 4.45%; N, 5.62%. Found: C, 66.35%; H, 4.51%; N, 5.58%.

### 2.7. Surface modification of ZnO nanoparticles

ZnO nanoparticles were preheated at 110 °C in a vacuum oven for 24 h to remove absorbed moisture and then were used for preparation of bionanocomposite. ZnO nanoparticles (0.2 g) were added into absolute ethanol (10 mL) and were ultrasonicated for 15 min. Then, KH570 or KH550 (20 wt% ZnO) was added to the dispersed solution, and the mixture of nanoparticles and silane coupling agents was irradiated under ultrasonic radiation for 30 min. The suspension was filtrated and washed with ethanol to remove unreacted KH570 or KH550 and the obtained solid was dried at 60 °C for more than 24 h.

### 2.8. Preparation of PAEI/ZnO BNCs

The preparation of PAEI/ZnO BNCs was carried out by the following procedure: different amounts of modified ZnO nanoparticles (6, 8 and 10 wt%) were mixed with PAEI (0.1 g) and the mixture was dispersed in 20 mL of absolute ethanol and then was irradiated under ultrasound waves for 4 h. The solvent was removed and the obtained solid was dried in vacuum at 80 °C for 4 h.

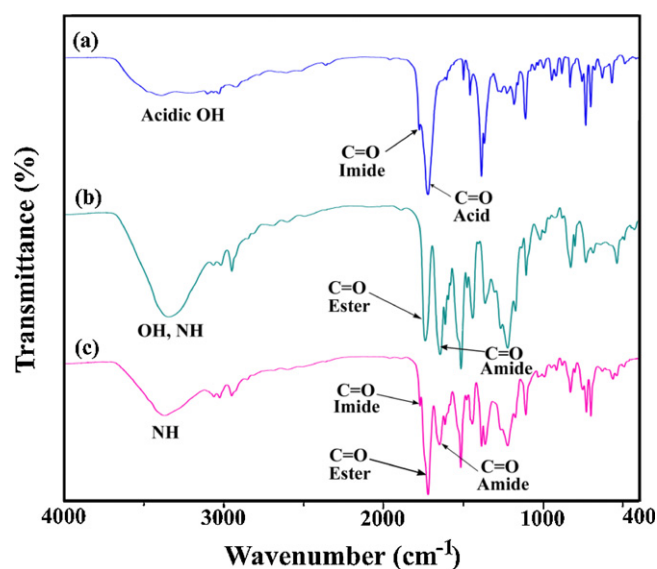
## 3. Results and discussion

### 3.1. Polymer synthesis

The optically active diol (**5**) and diacid (**9**) were synthesized according to the reported procedures [21,28]. PAEI **10** was

synthesized by direct polycondensation of an equimolar mixture of diol (**5**) with diacid (**9**) using TsCl/DMF/Py as a condensing agent (Scheme 3). The inherent viscosity of the resulting polymer was 0.39 dL/g and the yield was 68%. Because of the existence of amino acid in the polymer's backbone, this polymer is optically active and its specific rotation is  $[\alpha]_D^{25} = -8.76^\circ$  ( $c = 0.5$  g/dL, NMP).

The structure of synthesized polymer was confirmed by FT-IR, <sup>1</sup>H NMR spectroscopy and elemental analysis.

Fig. 1. FT-IR spectra of: (a) diacid **9**, (b) diol **5** and (c) PAEI.

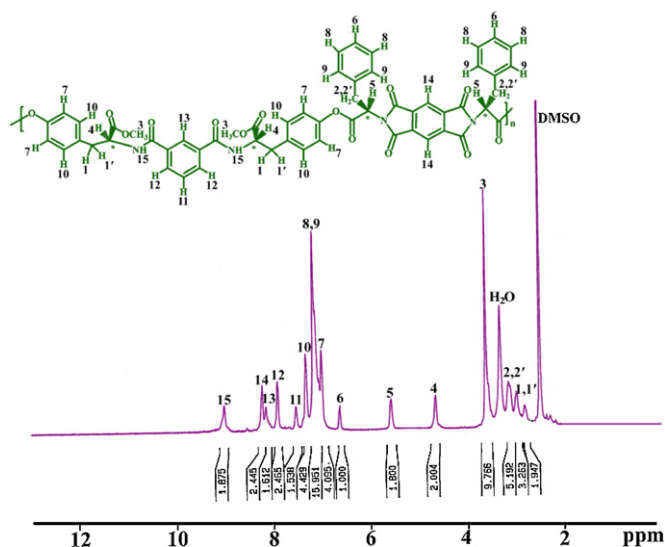


Fig. 2.  $^1\text{H}$  NMR spectrum of PAEI.

### 3.1.1. FT-IR analysis

The FT-IR spectrum of polymer (Fig. 1c) showed absorptions around  $3374\text{ cm}^{-1}$  (N–H), and three carbonyl (imide, ester and amide's C=O) absorptions at  $1771$ ,  $1721$  and  $1649\text{ cm}^{-1}$ , respectively. Absorptions at  $1385$  and  $727\text{ cm}^{-1}$  indicated the presence of the imide heterocycle in the polymer construction.

### 3.1.2. $^1\text{H}$ NMR study

The  $^1\text{H}$  NMR spectrum confirmed the structure of synthesized polymer (Fig. 2). The two different protons of chiral centers appeared at 4.62 and 4.53 ppm that is due to the existence of two kinds of amino acid in the PAEI structure. The peaks between 6.59 and 8.11 ppm were assigned to aromatic protons and the peak at 8.18 ppm was assigned to pyromellitimide ring protons. The N–H proton of amide groups appeared at 8.97 ppm.

According to our previous works, diol (5) and diacid (9) are biologically active and biodegradable in soil environment [21,29], therefore the synthesized PAEI is expected to be biodegradable and could be classified under environmentally friendly polymers.

### 3.1.3. Thermal properties (TGA and DSC analysis)

The thermal properties of PAEI were evaluated by TGA in a nitrogen atmosphere at a heating rate of  $10\text{ }^\circ\text{C}/\text{min}$  (Fig. 3). The temperature of 5% and 10% weight loss with char yield at  $800\text{ }^\circ\text{C}$  have been calculated from thermograms, and used to evaluate the thermal stability of the polymer. The 5 and 10% weight loss temperatures of the PAEI are  $279$  and  $298\text{ }^\circ\text{C}$ , respectively. The char yield of this polymer in  $\text{N}_2$  atmosphere is 27% at  $800\text{ }^\circ\text{C}$ . According

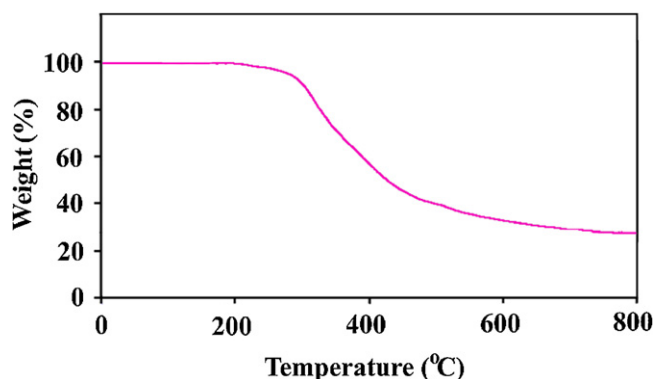


Fig. 3. TGA thermogram of PAEI.

to these data the synthesized polymer is thermally stable that is due to the existence of aromatic structure in the polymer's backbones which increases the stability of the polymer toward heating.

In addition, the thermal properties of the synthesized polymer were calculated via DSC measurement with a heating rate of  $10\text{ }^\circ\text{C}/\text{min}$  under nitrogen atmosphere. According to the obtained result, the glass transition temperature ( $T_g$ ) of this polymer was  $178\text{ }^\circ\text{C}$ .

### 3.1.4. Field emission scanning electron microscopy (FE-SEM)

The morphology of PAEI was studied via FE-SEM analysis. According to these micrographs (Fig. 4), the polymer consists of nano and sphere structure.

## 3.2. Bionanocomposites synthesis and characterization

At first, to improve the dispersion of nanoparticles and increasing possible interactions between nanoparticles and polymer matrix, the surface of the ZnO nanoparticles were modified with  $\gamma$ -methacryloxypropyltrimethoxy silane, KH570 and  $\gamma$ -aminopropyltriethoxy silane, KH550. The hydroxyl groups of ZnO were replaced with  $\text{OCH}_3$  of the KH570 or  $\text{OCH}_2\text{CH}_3$  of the KH550 to bond to its surface [11,30]. In functionalized ZnO, the organic chains of KH570 and KH550 can fulfill steric hindrance between inorganic nanoparticles and prevent their aggregation. Then, PAEI/ZnO BNCs were fabricated by adding various ZnO contents to the PAEI/EtOH suspension under ultrasound irradiation.

### 3.2.1. FT-IR study

Figs. 5 and 6 show the FT-IR spectra of pure PAEI, modified ZnO with two different coupling agents and bionanocomposites. The spectra of the novel BNCs with different ZnO-KH570 and

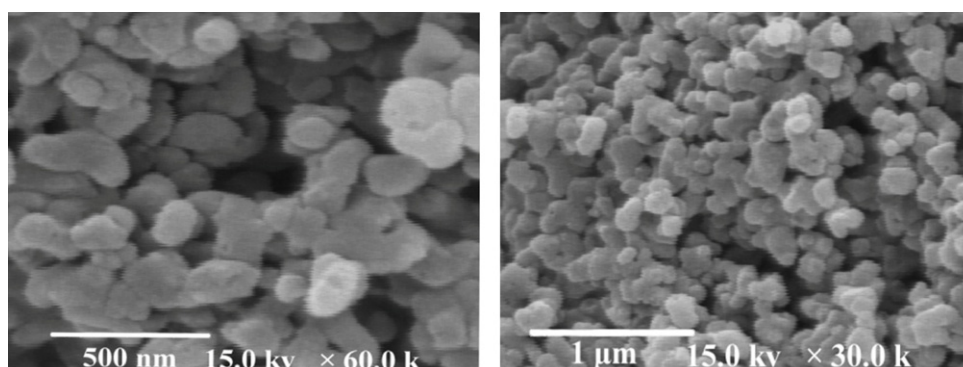


Fig. 4. FE-SEM micrographs of pure PAEI.

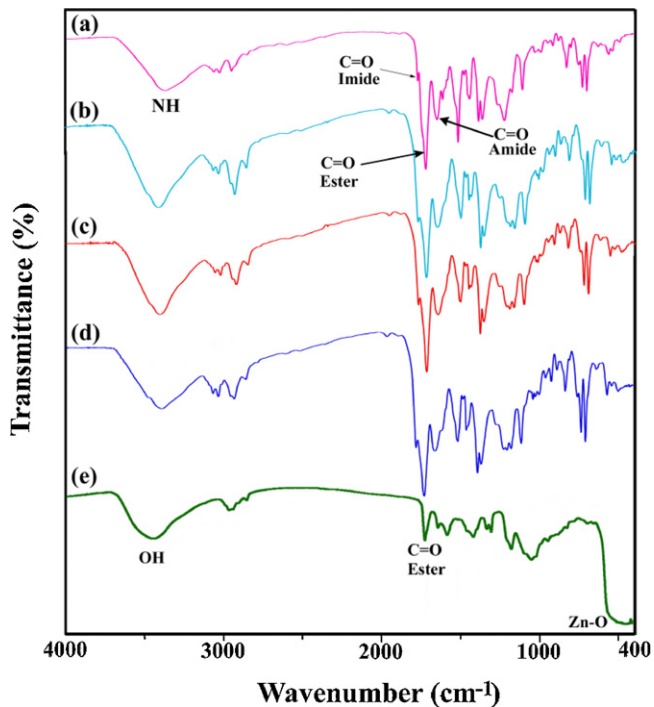


Fig. 5. FT-IR spectra of: (a) PAEI, (b) PAEI/ZnO-KH570 (6 wt%), (c) PAEI/ZnO KH570 (8 wt%), (d) PAEI/ZnO-KH570 (12 wt%) and (e) ZnO-KH570.

ZnO-KH570 contents [Figs. 5 and 6(b–d)] exhibit the characteristic absorption peaks corresponding to polymeric functional groups and ZnO nanoparticles. In BNCs spectra the appearance of a broad peak at around  $400\text{--}600\text{ cm}^{-1}$  which is related to Zn–O–Zn bonds, confirmed the interaction of ZnO with synthesized PAEI and also by increasing the amount of nanoparticles, the intensity of this peak was increased.

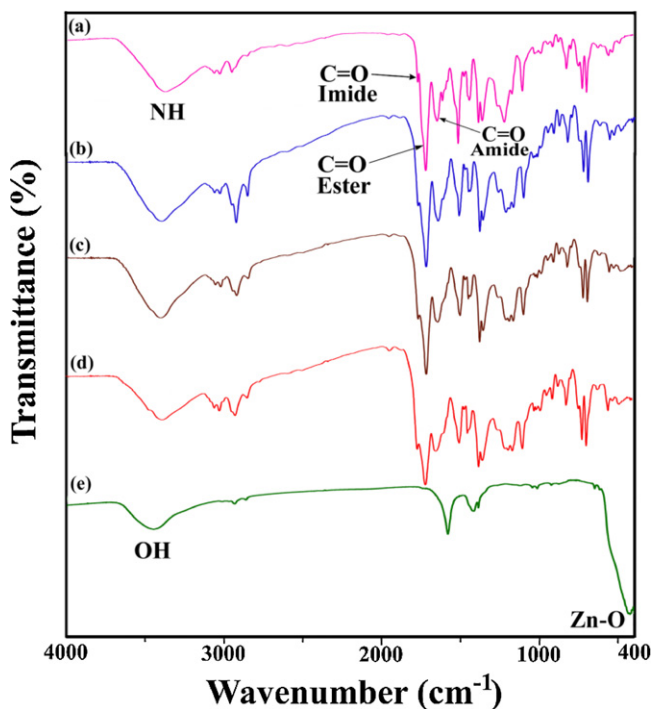


Fig. 6. FT-IR spectra of: (a) PAEI, (b) PAEI/ZnO-KH570 (6 wt%), (c) PAEI/ZnO-KH570 (8 wt%), (d) PAEI/ZnO-KH570 (12 wt%) and (e) ZnO-KH570.

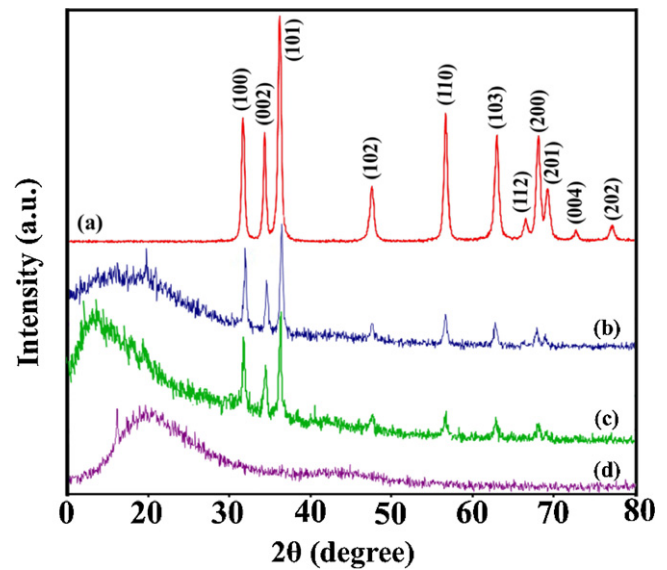


Fig. 7. XRD spectra of: (a) ZnO, (b) PAEI/ZnO-KH570 (10 wt%), (c) PAEI/ZnO-KH570 (10 wt%) and (d) PAEI.

### 3.2.2. X-ray diffraction (XRD) analysis

The XRD patterns of PAEI, PAEI/ZnO-KH570 (10 wt%), PAEI/ZnO-KH570 (10 wt%) and ZnO are shown in Fig. 7. Pure PAEI with no sharp diffraction peaks is completely amorphous in nature (Fig. 7d). Fig. 7b and c shows the XRD patterns of BNCs with 10 wt% of ZnO-KH570 and ZnO-KH570, which indicate that the morphology of ZnO nanoparticles was not changed during the process. In Fig. 7a, a series of characteristic peaks: (1 0 0), (0 0 2), (1 0 1), (1 0 2), (1 1 0), (1 0 3), (2 0 0), (1 1 2), (2 0 1), (0 0 4) and (2 0 2) are noticed, which are in accordance with the zincite phase of ZnO (International Center for diffraction data, JCPDS No. 36-1451).

### 3.2.3. Thermal properties (TGA and DSC analysis)

The thermal properties of BNCs were investigated by TGA. The thermal gravimetric profiles of the BNCs (10 wt%) are shown in Fig. 8. The thermal stability of both BNCs was increased compared to pure polymer. This improvement in thermal stability may be caused by the fact that the ZnO nanoparticles have larger surface area which improves the thermal cover or preventing out-diffusion of the volatile decomposition products.

Furthermore, the thermal properties of both BNCs (10 wt%) were examined by DSC. The glass transition temperature ( $T_g$ ) of the bionanocomposites was decreased with respect to pure PAEI. The  $T_g$  for PEA/ZnO-KH570 (10 wt%) and PEA/ZnO-KH570 (10 wt%) is

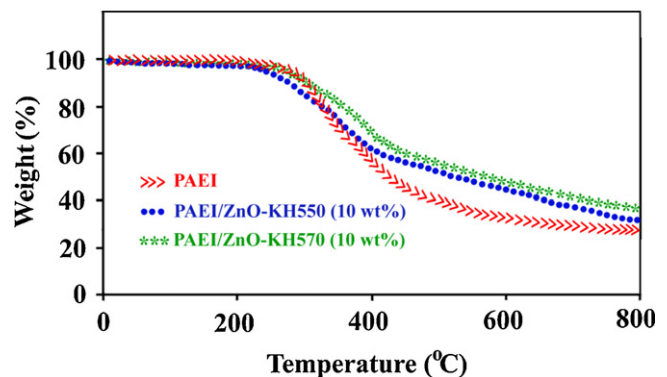


Fig. 8. TGA thermograms of PAEI, PEA/ZnO-KH570 (10 wt%) and PEA/ZnO-KH570 (10 wt%) under a nitrogen atmosphere at heating rate of  $10\text{ °C/min}$ .

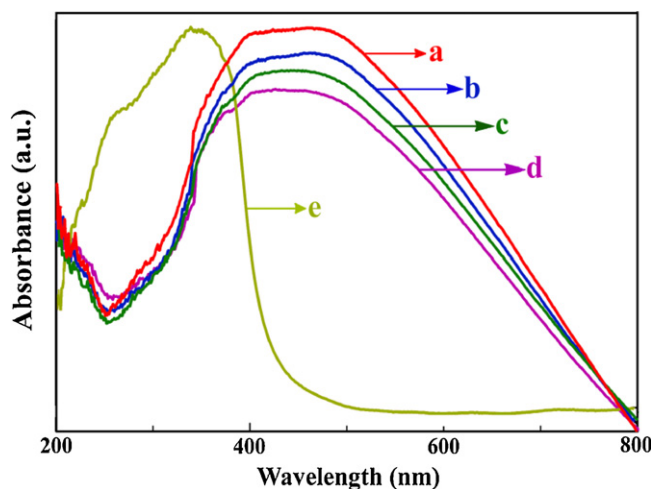


Fig. 9. UV/vis spectra of: (a) PAEI, (b) PAEI/ZnO-KH570 (6 wt%), (c) PAEI/ZnO-KH570 (8 wt%), (d) PAEI/ZnO-KH570 (12 wt%) and (e) ZnO-KH570.

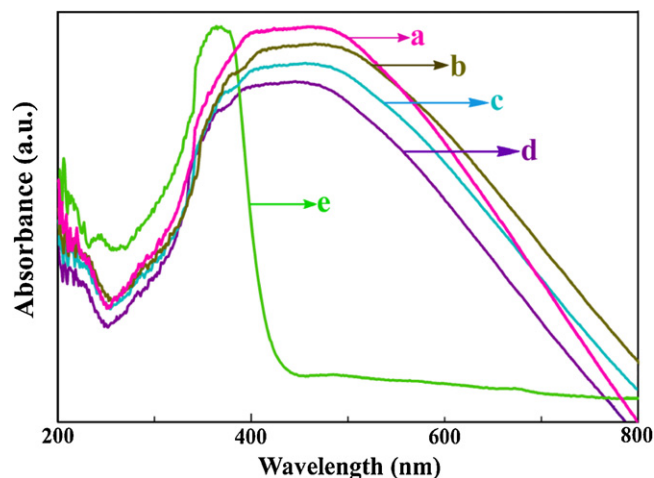


Fig. 10. UV/vis spectra of: (a) PAEI, (b) PAEI/ZnO-KH550 (6 wt%), (c) PAEI/ZnO-KH550 (8 wt%), (d) PAEI/ZnO-KH550 (12 wt%) and (e) ZnO-KH550.

160 and 167 °C, respectively. The DSC results showed the effect of nanoparticles on the reaction between polymer chains and modified ZnO nanoparticles. These results indicate that the polymer chain mobility is enhanced in the presence of the filler because of increasing the hydrogen bonding between polymer and functionalized ZnO, while the hydrogen bonding between PAEI and PAEI is decreased, so the  $T_g$  of BNCs is reduced.

#### 3.2.4. UV/vis absorption

The UV/vis absorption of ZnO-KH570, PAEI/ZnO-KH570 BNCs and PAEI are shown in Fig. 9 and the UV/vis absorption of ZnO-KH550, PAEI/ZnO-KH550 BNCs and PAEI are shown in Fig. 10. Pure PAEI displays absorbance in the UV region due to its delocalized  $\pi$ -electrons and shows the maximum absorption peak at 459 nm (Figs. 9a and 10a). The ZnO-KH570 and ZnO-KH550 show maximum UV absorption peak at 338 and 368 nm, respectively (Figs. 9e and 10e). In two different BNCs groups, by increasing of ZnO contents, the maximum absorption peak of polymer is shifted to the maximum absorption peak of modified ZnO nanoparticle. The obtained BNCs have absorption around the UV region, so it is

expected that these materials can be used as a UV shielding materials.

#### 3.2.5. Morphology studies

FE-SEM images of bionanocomposites were taken to study the morphological features and the representative images of 10 wt% PAEI/ZnO-KH570 and 10 wt% PAEI/ZnO-KH550 bionanocomposites were displayed in Fig. 11. These images show that ZnO nanoparticles were dispersed homogeneously in nano scale in polymer matrix.

According to these micrographs, KH570 modified ZnO nanoparticles (Fig. 11a and b), disperse better than the one which was modified with KH550 (Fig. 11d and e) and also the size of particles are smaller. For KH550 coupling agent, the functional group which provides different interactions to ZnO nanoparticle is the amino group. Various interactions between aminosilane and ZnO surface were proposed as follows: (a) hydrogen bonding; (b) ionic bonding; (c) covalent bonding with surface hydroxyl groups [31–33]. Due to these interactions, the aggregation of nanoparticles is more when ZnO is modified with KH550, so the distance

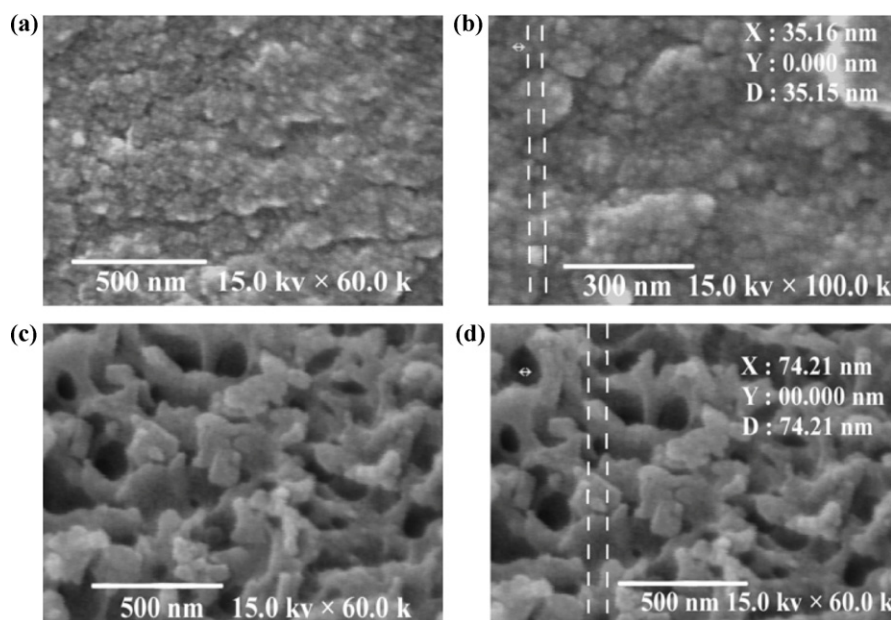


Fig. 11. FE-SEM micrographs of (a and b) PAEI/ZnO-KH570 (10 wt%) and (c and d) PAEI/ZnO-KH550 (10 wt%).

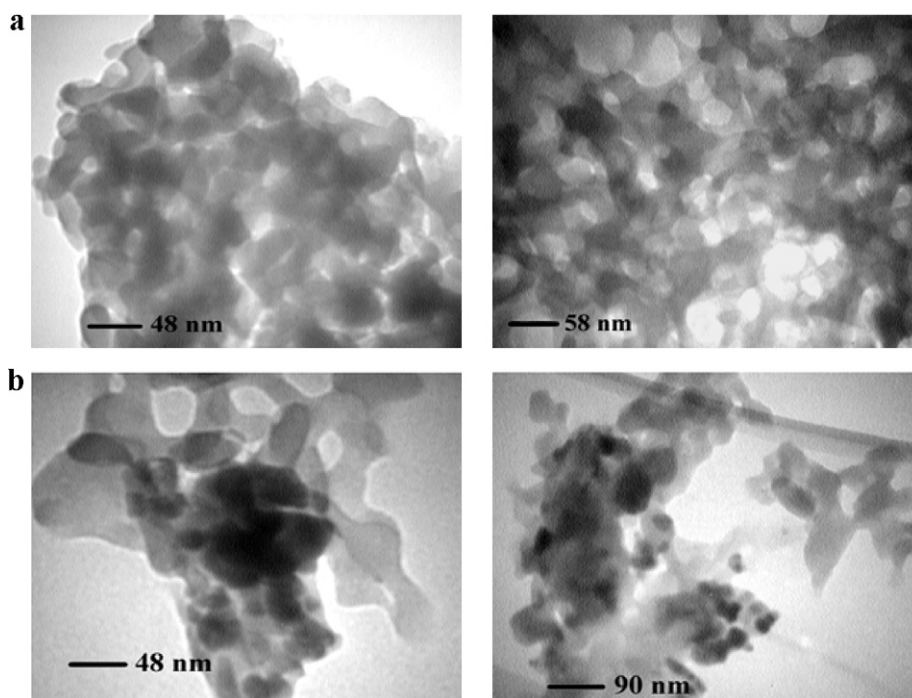


Fig. 12. TEM micrographs of (a) PAEI/ZnO-KH570 (10 wt%) and (b) PAEI/ZnO-KH550 (10 wt%).

between polymer's chains is increased and the homogeneous dispersion is reduced and the morphology of PAEI/ZnO-KH550 BNC seems to be spongy (Fig. 11c).

TEM micrographs of PAEI/ZnO-KH570 and PAEI/ZnO-KH550 BNCs with 10 wt% ZnO are shown in Fig. 12a and b, respectively. TEM indicated that the ZnO particles were well dispersed in the polymer matrix in nano scale, representing that the coupling agents play an important role in dispersing the nanoparticles.

#### 4. Conclusion

A novel optically active, biodegradable and nanostructured PAEI was successfully synthesized through direct polycondensation of amino acid based diol and diacid. The synthesized polymer was thermally stable and shows nanostructure. PAEI/ZnO BNCs were fabricated via embedding ZnO nanoparticles into PAEI matrix by ultrasound irradiation process. The surface of ZnO was modified with two different silane coupling agents (KH570 and KH550), to achieve a uniform dispersity of ZnO nanoparticles in polymer matrix. Surface-treating ZnO nanoparticles with the suitable modifying agents, increase the compatibility of ZnO particles with PAEI matrix, and also efficiently improved the thermal stability of the PAEI/ZnO bionanocomposites. Finally, based on TEM and FE-SEM results and according to the type of interactions it seems that KH570 linker was more effective than KH550.

#### Acknowledgements

We gratefully acknowledge the partial financial support from the Research Affairs Division Isfahan University of Technology (IUT), Isfahan. Further partial financial support of Iran Nanotechnology Initiative Council (INIC), National Elite Foundation (NEF) and Center of Excellence in Sensors and Green Chemistry (IUT) is also gratefully acknowledged.

#### References

- [1] K. Tada, M. Onoda, *Thin Solid Films* 438–439 (2003) 365.
- [2] L. Dai, in: H.S. Nalwa (Ed.), *Encyclopedia of Nanoscience and Nanotechnology*, American Scientific Publishers, 2004, p. 763.
- [3] S. Shang, L. Li, X. Yang, L. Zheng, *J. Colloid Interface Sci.* 333 (2009) 415.
- [4] J.D. Patel, T.K. Chaudhuri, *Mater. Res. Bull.* 44 (2009) 1647.
- [5] C. Wei, Y. Zhu, Y. Jin, X. Yang, C. Li, *Mater. Res. Bull.* 43 (2008) 3263.
- [6] Z. Guo, S. Wei, B. Shedd, R. Scaffaro, T. Pereira, H.T. Hahn, *J. Mater. Chem.* 17 (2007) 806.
- [7] A.P. Kumar, D. Depan, N. Singh Tomer, R.P. Singh, *Prog. Polym. Sci.* 34 (2009) 479.
- [8] N.G. Semaltianos, S. Logothetidis, N. Hastas, W. Perrie, S. Romani, R.J. Potter, G. Dearden, K.G. Watkins, P. French, M. Sharp, *Chem. Phys. Lett.* 484 (2010) 283.
- [9] Rajesh, T. Ahuja, D. Kumar, *Sens. Actuators B: Chem.* 136 (2009) 275.
- [10] S. Yang, Y. Ishikawa, H. Itoh, Q. Feng, *J. Colloid Interface Sci.* 356 (2011) 734.
- [11] E. Tang, B. Tian, E. Zheng, C. Fu, G. Cheng, *Chem. Eng. Commun.* 195 (2008) 479.
- [12] M.Z. Rong, M.Q. Zhang, H.B. Wang, H.M. Zeng, *Appl. Surf. Sci.* 200 (2002) 76.
- [13] Z. Li, Y. Zhu, *Appl. Surf. Sci.* 211 (2003) 315.
- [14] F. Bauer, H. Ernst, U. Decker, M. Findeisen, H.-J. Gläsel, H. Langguth, E. Hartmann, R. Mehnert, C. Peuker, *Macromol. Chem. Phys.* 201 (2000) 2654.
- [15] F. Bauer, H.-J. Gläsel, U. Decker, H. Ernst, A. Freyer, E. Hartmann, V. Sauerland, R. Mehnert, *Prog. Org. Coat.* 47 (2003) 147.
- [16] M. Fuji, T. Takei, T. Watanabe, M. Chikazawa, *Colloids Surf. A: Physicochem. Eng. Aspects* 154 (1999) 13.
- [17] E. Ruiz-Hitzky, M. Darder, P. Aranda, *J. Mater. Chem.* 15 (2005) 3650.
- [18] L. Petersson, K. Oksman, *Compos. Sci. Technol.* 66 (2006) 2187.
- [19] M. Okada, *Prog. Polym. Sci.* 27 (2002) 87.
- [20] N.A. Kumar, A. Bund, B.G. Cho, K.T. Lim, Y.T. Jeong, *Nanotechnology* 20 (2009) 225608.
- [21] A. Abdolmaleki, S. Mallakpour, S. Borandeh, M. Sabzalian, *Amino Acids* (2011), doi:10.1007/s00726-011-0931-1.
- [22] S. Mallakpour, P. Asadi, M.R. Sabzalian, *Amino Acids* (2010), doi:10.1007/s00726-010-0799-5.
- [23] R.A. Hule, D.J. Pochan, *Mater. Res. Bull.* 32 (2007) 354.
- [24] S. Mallakpour, S. Soltanian, *Polymer* 51 (2010) 5369.
- [25] N. Saha, A.K. Dubey, B. Basu, *J. Biomed. Mater. Res. B: Appl. Biomater.* 100B(2012)256.
- [26] N. Saha, K. Keskinbora, E. Suvaci, B. Basu, *J. Biomed. Mater. Res. B: Appl. Biomater.* 95B (2010) 430.
- [27] A. Nagai, J. Ishikawa, H. Kudo, T. Endo, *J. Polym. Sci. A: Polym. Chem.* 42 (2004) 1143.
- [28] S.E. Mallakpour, A.-R. Hajipour, S. Habibi, *J. Appl. Polym. Sci.* 86 (2002) 2211.
- [29] S. Mallakpour, S. Soltanian, M. Sabzalian, *J. Polym. Res.* (2011), doi:10.1007/s10965-011-9573-y.
- [30] E. Tang, H. Liu, L. Sun, E. Zheng, G. Cheng, *Eur. Polym. J.* 43 (2007) 4210.
- [31] N.R.E.N. Impens, P. van der Voort, E.F. Vansant, *Microporous Mesoporous Mater.* 28 (1999) 217.
- [32] C.-H. Chiang, H. Ishida, J.L. Koenig, *J. Colloid Interface Sci.* 74 (1980) 396.
- [33] E. Ukaji, T. Furusawa, M. Sato, N. Suzuki, *Appl. Surf. Sci.* 254 (2007) 563.